第 29 卷第 7 期 无 机 化 学 学 报 Vol.29 No.7
2013 年 7 月 CHINESE JOURNAL OF INORGANIC CHEMISTRY 1504-1512

以 5-甲基-3-吡唑甲酸为配体构建的具有六方孔道的钴(Ⅱ)、镍(Ⅱ)超分子化合物:合成、晶体结构和性质

包金婷[1] 程美令[1] 刘 琦*[,1,2] 韩 伟[1] 纪云洲[1] 翟长伟[1] 洪 健[1] 孙小强*[1]
([1]常州大学石油化工学院,江苏省精细石油化工重点实验室,常州 213164)
([2]南京大学配位化学国家重点实验室,南京 210093)

摘要:利用 5-甲基-3-吡唑甲酸,分别与 $CoCl_2\cdot 6H_2O$ 和 $Ni(NO_3)_2\cdot 6H_2O$ 反应,得到了配合物[$M(MPA)_2(H_2O)_2$](**1**:M=Co;**2**:M=Ni)(HMPA=5-甲基-3-吡唑甲酸)。用元素分析、红外光谱、X-单晶衍射结构分析对其进行了表征。配合物 **1** 和 **2** 的晶体结构参数如下:配合物 **1** 和 **2** 的晶体都属于六方晶系,空间群为 $R\bar{3}c$。配合物 **1** 的晶胞参数为 a=1.483 94 (4) nm,b=1.483 94 (4) nm,c=3.207 66(6) nm,V=6.117 2(3) nm^3,Z=18;配合物 **2** 的晶胞参数为 a=1.466 53(14) nm,b=1.466 53(14) nm,c=3.243 0(6) nm,V=6.04 03(14) nm^3,Z=18。金属离子与来自 2 个 5-甲基-3-吡唑甲酸配体中的 2 个氮原子及 2 个氧原子,2 个水分子中的 2 个氧原子配位,形成八面体配位构型。配合物中的独立结构单元[$M(MPA)_2(H_2O)_2$]通过分子间氢键形成具有六方孔道的三维结构。热重分析表明配合物 **1** 和 **2** 具有较高的热稳定性。此外,考察了配合物 **1** 和 **2** 的荧光和电化学性质。CCDC: 900677,**1**;900678,**2**。

关键词:钴;镍;5-甲基-3-吡唑甲酸;晶体结构;荧光性质;电化学性质
中图分类号:O614.81$^+$2;O614.81$^+$3 **文献标识码**:A **文章编号**:1001-4861(2013)07-1504-09
DOI: 10.3969/j.issn.1001-4861.2013.00.215

Cobalt and Nickel Supramolecular Complexes with Hexagonal Channels Constructed from 5-Methyl-1*H*-Pyrazole-3-Carboxylic Acid: Synthesis, Crystal Structures and Properties

BAO Jin-Ting[1] CHENG Mei-Ling[1] LIU Qi*[,1,2] HAN Wei[1] JI Yun-Zhou[1] ZHAI Chang-Wei[1]
HONG Jian[1] SUN Xiao-Qiang*[,1]
([1]*School of Petrochemical Engineering and Jiangsu Province Key Laboratory of Fine Petro-chemical Technology, Changzhou University, Changzhou, Jiangsu* 213164, *China*)
([2]*State Key Laboratory of Coordination Chemistry, Nanjing University, Nanjing* 210093, *China*)

Abstract: The new monomeric complexes of [$M(MPA)_2(H_2O)_2$] (**1**: M=Co; **2**: M=Ni) (HMPA=5-methyl-1*H*-pyrazole-3-carboxylic acid) were synthesized by the reaction of 5-methyl-1*H*-pyrazole-3-carboxylic acid with $CoCl_2\cdot 6H_2O$ and $Ni(NO_3)_2\cdot 6H_2O$, respectively. The compounds were characterized by elemental analysis, IR spectra, single crystal X-ray diffraction. The structural parameters of **1** and **2** were analyzed as follows: **1**, Hexagonal, $R\bar{3}c$, a=1.48394 (4) nm, b=1.483 94 (4) nm, c=3.207 66 (6) nm, V=6.1172 (3) nm^3, Z=18; **2**, Hexagonal, $R\bar{3}c$, a=1.466 53(14) nm, b=1.466 53(14) nm, c=3.243 0(6) nm, V=6.040 3(14) nm^3, Z=18. Metal ions have all octahedral geometry coordinated by two nitrogen atoms and two oxygen atoms from two MPA^- ligands, two oxygen atoms from two H_2O molecules. In both complexes, the independent components [$M(MPA)_2(H_2O)_2$] are connected by intermolecular hydrogen bonds to form a three-dimensional architecture with hexagonal channels. Thermogravimetric analyses show that **1** and **2** have higher thermal stability. In addition, the luminescent properties and electrochemical properties of complexes **1** and **2** have also been investigated. CCDC: 900677, **1**; 900678, **2**.

Key words: cobalt(Ⅱ); nickel(Ⅱ); 5-methyl-1*H*-pyrazole-3-carboxylic acid; crystal structure; luminescent property; electrochemical property

收稿日期:2012-11-26。收修改稿日期:2013-02-25。
国家自然科学基金(No.20971060; 21101018);南京大学配位化学国家重点实验室开放基金;江苏高校优势学科建设工程资助项目。
*通讯联系人。E-mail:liuqi62@163.com; chemsxq@yahoo.com.cn;;会员登记号:S060018987P。

0 Introduction

Recently, much effort has been focused on synthesis of new functional supramolecular complexes of novel topologies, due to their enormous variety of intriguing structural topology and the potential applications in magnetism, chirality, molecular adsorption, luminescent materials, separations and catalysis and so forth [1-8]. Meanwhile, supramolecular complexes can be considered as true space extend network formed through intermolecular weak interactions such as hydrogen bonding, vander Waals, π-π stacking, and electrostatic interactions [9-12]. In particular, the self-assembly of supramolecular complexes is mainly inuenced by various factors such as organic ligands, metal ions, solvent systems, and pH value, etc. Therefore, proper selection of metal ions and organic ligands is a key issue in designing and self-assembly of new functional supramolecules [13-16]. In order to create such supramolecular complexes, a rigid ligand with multiple coordination sites is demanded. Heterocyclic carboxylic acids ligands with rigidly frames, such as pyridinecarboxylic acid [17-20], pyrazolecarboxylic acid [21-23], and imidazolecarboxylic acid[24-26], pyrazinecarboxylic acid[27-28] and so forth, are versatile ligands due to their multi-coordination mode by the N and O donor atoms on the heterocyclic rings and the carboxyl groups. Among them, pyrazolecarboxylic acid ligands have emerged as a new kind of ligands promising for assembling supramolecular networks. As protons donors and acceptors, the pyrazole nitrogen atoms and carboxylic oxygen atoms in pyrazolecarboxylic acids not only can coordinate with metals ions to form monodentate and/or multidentate M-N and M-O bonds, but also provide intermolecular hydrogen bonds for assembling the complex into high-dimensional networks. 5-methyl-3-pyrazolecarboxylic acid (HMPA) is such a multifunctional ligand. However, studies of complexes containing HMPA ligand are rare [29-31], especially, researches of constructing supramolecular network structures with hexagonal topology [32-33] using HMPA ligand have not been explored so far. Herein, as the continuation of our research in constructing supramolecular compounds based on HMPA, we report the synthesis and hexagonal supramolecular structures of the complexes $[M(MPA)_2(H_2O)_2]$ (**1**: M=Co; **2**: M=Ni). In addition, IR spectra, thermal decomposition, luminescent properties and electrochemical properties will be discussed.

1 Experimental

1.1 Materials and methods

All solvents and starting materials for synthesis were purchased commercially and were used as received unless otherwise noted. 5-methyl-1H-pyrazole-3-carboxylic acid (HMPA) was synthesized and purified according to the modified literature method[34]. The elemental analysis (C, H and N) was performed on a Perkin-Elmer 2400 Series II element analyzer. FTIR spectra were recorded on a Nicolet 460 spectrophotometer in the form of KBr pellets. Single-crystal X-ray diffraction measurement of the title compounds were carried out with a Bruker Smart Apex II CCD diffractometer at 293 (2) K. Thermogravimetric analysis (TGA) experiments were carried out on a Dupont thermal analyzer at a heating rate of 10 ℃·min^{-1} under N_2 atmosphere. Electrochemical property was carried out on CHI660 D electrochemical analyzer (Beijing Huake Putian Science and Technology Co. Ltd) in highly pure nitrogen atmosphere. A Pt-piece was employed as working electrode, a saturated calomel electrode (SCE) as reference electrode and a platinum wire as auxiliary electrode. The supporting electrolyte was 0.1 mol·L^{-1} NaCl. The half wave potentials $E_{1/2}$ were obtained from $(E_{pa}+E_{pc})/2$. Luminescence spectra of solid samples were recorded on a Varian Cary Eclipse spectrometer.

1.2 Synthesis

1.2.1 Preparation of $[Co(MPA)_2(H_2O)_2]$(**1**)

To a solution containing HMPA (0.012 6 g, 0.1 mmol) in EtOH (5 mL) was added a solution of $CoCl_2\cdot 6H_2O$ (0.023 8 g, 0.1 mmol) in water (3 mL). The resulting solution was stirred for one hour and allowed to stand at room temperature for two weeks. Orange

square crystals of **1** suitable for X-ray diffraction analysis were obtained. Anal. Calcd. for $C_{10}H_{14}CoN_4O_6$ (%): C, 34.76; H, 4.06; N, 16.22. Found (%): C, 34.35; H, 4.21; N, 16.41. IR spectrum (cm^{-1}, KBr pellet): 3 481 (m), 3 132 (w), 2 964 (w), 2 855 (w), 1 608 (s), 1 568 (w), 1 548 (w), 1 499 (s), 1 423 (vs), 1 386 (m), 1 352 (vs), 1 291 (m), 1 200 (m), 1 126 (w), 1 046 (w), 1 019 (s), 984 (w), 841 (vs), 825 (w), 795 (w), 691 (m), 648 (w), 557 (w), 446 (m).

1.2.2 Preparation of $[Ni(MPA)_2(H_2O)_2]$(**2**)

HMPA (0.025 2 g, 0.2 mmol) and $Ni(NO_3)_2\cdot 6H_2O$ (0.037 7 g, 0.13 mmol) were added into 20 mL deionized water and stirred for 30min, then the pH value of the green solution was adjusted to 8.0 with KOH solution(0.1 $mol\cdot L^{-1}$) and further stirred for 3 h. The resulting solution was evaporated at room temperature slowly. Green block crystals of **2** suitable for X-ray diffraction analysis were obtained. Anal. Calcd. for $C_{10}H_{14}NiN_4O_6$ (%): C, 34.54; H, 4.09; N, 16.24. Found (%):C, 34.32; H, 4.16; N, 16.44. IR spectrum (cm^{-1}, KBr pellet): 3493 (m), 3175 (w), 2957 (w), 2848 (w), 1610 (s), 1550 (w), 1503 (s), 1427 (s), 1390 (m), 1354 (s), 1294 (vs), 1207 (vs), 1127 (w), 1046 (w), 1024 (m), 1017 (w), 984 (w), 904 (w), 841 (s), 794 (w), 693 (m), 647(w), 562 (w), 451 (m).

1.3 X-ray crystallography

Single-crystal X-ray diffraction measurement of the compounds **1** and **2** were carried out with a Bruker Smart Apex II CCD diffractometer at 293(2) K. Intensities of reflections were measured using graphite-monochromatized Mo $K\alpha$ radiation (λ=0.071 073 nm) with the φ-ω scans mode in the range of $2.03° \leqslant \theta \leqslant 24.99°$ (for **1**) and $2.00° \leqslant \theta \leqslant 27.6°$ (for **2**). The structure was solved by direct methods using SHELXS-97[35] computer program and refined by full-matrix least-squares methods on F^2 with the SHELXL-97 program package. Anisotropic thermal factors were assigned to all the non-hydrogen atoms. H atoms attached to C were placed geometrically and allowed to ride during subsequent refinement with an isotropic displacement parameter fixed at 1.2 times Ueq of the parent atoms. H atoms bonded to O or N were first located in difference Fourier maps and then placed in the calculated sites and included in the refinement. Crystallographic data parameters for structural analyses are summarized in Table 1.

Table 1 Crystal structure parameters of the title complexes

Compound	**1**	**2**
Empirical formula	$C_{10}H_{14}CoN_4O_6$	$C_{10}H_{14}N_4NiO_6$
Formula mass	345.18	344.96
Color	Orange	Green
Crystal size / mm	0.22×0.20×0.18	0.24×0.22×0.20
Temperature / K	293(2)	293(2)
Wavelength / nm	0.071 073	0.071 073
Crystal system	Hexagonal	Hexagonal
Space group	$R\bar{3}c$	$R\bar{3}c$
a / nm	1.483 94(4)	1.466 53 (14)
b / nm	1.483 94(4)	1.466 53 (14)
c / nm	3.207 66(6)	3.243 0 (6)
α / (°)	90.00	90.00
β / (°)	90.00	90.00
γ / (°)	120.00	120.00
V / nm^3	6.117 2(3)	6.040 3(14)
Z	18	18
D_c / ($g\cdot cm^{-3}$)	1.687	1.707
μ(Mo $K\alpha$) / mm^{-1}	1.297	1.480

Continued Table 1

Index ranges(h, k, l)	−17/16, −15/17, −30/38	−18/19, −19/15, −31/42
F(000)	3186	3204
θ range for data collection / (°)	2.03 to 24.99	2.04 to 27.57
Reflections collected	10 693	12 115
Independent reflections (R_{int})	1 207(0.055)	1 557(0.097)
Observed reflections	1 149	1 178
Refinement method	Full-matrix least-squares on F^2	
Data / restraints / parameters	1 207/3/99	1 555/3/97
Goodness-of-fit on F^2	1.019	1.032
R_1, $wR_2[I>2\sigma(I)]$	0.026 0, 0.065 3	0.066 8, 0.127 8
R_1, wR_2 (all data)	0.036 7, 0.067 7	0.045 6, 0.114 4
Largest diff. Peak and hole / (e·nm^{-3})	540, −111 0	410, −680

Table 2 Selected bond lengths (nm) and angles (°) for complexes 1 and 2

Complex **1**					
Co1-O1	0.210 41(13)	Co1-O5A	0.208 38(14)	Co1-O1A	0.210 41(13)
Co1-N1	0.212 32(15)	Co1-O5	0.208 38(14)	Co1-N1A	0.212 32(15)
O5-Co1-O5A	88.14 (9)	O1A-Co1-N1A	77.77(5)	O5-Co1-O1A	88.98(6)
O1-Co1-N1A	91.09(5)	O5A-Co1-O1A	172.73(6)	O5-Co1-N1	95.89(6)
O5-Co1-O1	172.73(6)	O5A-Co1-N1	95.85(6)	O5A-Co1-O1	88.99(6)
O1A-Co1-N1	91.08(5)	O1A-Co1-O1	94.63(8)	O1-Co1-N1	77.77(5)
O5-Co1-N1A	95.84(6)	N1A-Co1-N1	163.64(8)	O5A-Co1-N1A	95.89(6)
Complex **2**					
Ni1-O3A	0.206 8 (2)	Ni1-N2	0.206 6 (3)	Ni1-N2A	0.206 6 (3)
Ni1-O3	0.206 8 (2)	Ni1-O1	0.207 4 (2)	Ni1-O1A	0.207 4 (2)
N2A-Ni1-N2	163.57 (15)	N2A-Ni1-O3A	96.22 (9)	N2-Ni1-O3A	95.67 (9)
N2A-Ni1-O3	95.67 (9)	N2-Ni1-O3	96.22 (9)	O3A-Ni1-O3	87.06 (14)
N2A-Ni1-O1	90.02 (10)	N2-Ni1-O1	78.98 (9)	O3A-Ni1-O1	88.60 (10)
O3-Ni1-O1	173.19 (9)	N2A-Ni1-O1A	78.98 (9)	N2-Ni1-O1A	90.01 (10)
O3A-Ni1-O1A	173.18 (9)	O3-Ni1-O1A	88.59 (10)	O1-Ni1-O1A	96.20 (14)

Symmetry codes: A: $x-y+1/3$, $-y+2/3$, $-z+1/6$ for **1**; A: $1/3+x$, $2/3+y$, $1/6-z$ for **2**

Table 3 Bond lengths (nm) and angles (°) of hydrogen bonds in 1 and 2

D-H···A	d(D-H) / nm	d(H···A) / nm	d(D···A) / nm	∠DHA / (°)
Complex **1**				
N2-H2···O2B	0.087	0.203	0.288 1(2)	166
O5-H5X···O2B	0.091	0.202	0.289 8(2)	163
O5-H5Y···O2C	0.094	0.177	0.270 5(2)	171
N1-H1···O2B	0.093	0.192	0.283 2 (4)	165
Complex **2**				
O3-H3X···O2B	0.095	0.201	0.292 7(3)	163
O3-H3Y···O2C	0.082	0.190	0.272 3(3)	175
O5-H5Y···O2C	0.094	0.177	0.270 5(2)	171

Symmetry codes: B: $2/3-y$,$1/3-x$, $-1/6+z$; C: $2/3-x+y$, $1/3+y$, $-1/6+z$ for **1**; B: $2/3-y$, $1/3-x$, $-1/6+z$; C: $2/3-x+y$, $1/3+y$, $-1/6+z$ for **2**

2 Results and discussion

2.1 Synthesis and IR spectra

Complex **1** was obtained by slow evaporation of EtOH-H_2O solution of HMPA and $CoCl_2 \cdot 6H_2O$ in a molar ratio of 1∶1; complex **2** was obtained by slow evaporation of aqueous solution of HMPA and $Ni(NO_3)_2 \cdot 6H_2O$ in a molar ratio of 2∶1.3 under adjusting pH=8, but the powder of Ni complex was only obtained by slow evaporation of EtOH-H_2O solution of HMPA and $NiCl_2 \cdot 6H_2O$ in a molar ratio of 1∶1; The complexes **1** and **2** are stable in air (via IR spectra analysis and elemental analysis), soluble partly in H_2O, and insoluble in C_2H_5OH, CH_3CN, DMF and ether.

The IR spectrum of **1** and **2** are similar (see Supplementary materials Figures S1-2), the strong and broad absorption bands around 3 000~3 500 cm^{-1} region in **1** and **2** are assigned as characteristic peaks of OH vibration, indicating that water molecules exist in both of them. Moreover, the strong peaks appearing at 1 548 cm^{-1} in **1** and 1 503 cm^{-1} in **2** are attributed to the stretching vibrations of C=N. The absorption peak between 1 690 cm^{-1} and 1 730 cm^{-1} is not observed, showing all carboxylic groups are deprotonated in **1** and **2**. For **1**, the strong peaks at 1 608 cm^{-1} and 1 386 cm^{-1} are the ν_{as} (COO^-), and ν_s (COO^-) stretching mode of the coordinated MPA^- ligand, respectively, while for **2**, the peaks at 1 610 cm^{-1} and 1 354 cm^{-1} belong to the ν_{as} (COO^-) and ν_s (COO^-) respectively. The different values between ν_{as} (COO^-) and ν_s(COO^-) of **1** and **2** are 222 cm^{-1} and 256 cm^{-1} respectively, which indicate that the carboxylates of MPA^- ligands adopt monodentate coordination[36-38] as proved by the X-ray crystal structure analysis of them.

2.2 Structural description of $[M(MPA)_2(H_2O)_2]$ (1: M=Co; 2: M=Ni)

The crystal structures of **1** and **2** are isostructural (Figures 1, 2 and 3 show the structure of **1**). Therefore, only the structure of complex **1** will be discussed in detail. As shown in Fig.1, the coordination sphere of each metal ion is defined by two oxygen atoms O1A, O1 and two nitrogen atoms N1A, N1 from the two MPA^- ligands as well as two oxygen atoms O5A, O5 from the two H_2O molecules, leading to an octahedral geometry. The bond angles of O1A-Co1-O1, O5A-Co1-O1, O5-Co1-O1A, O5-Co1-O5A are add up to equal to 360.74°(Table 2), showing that O1, O1A, O5 and O5A atoms are in the equatorial position. Moreover, the bond angles of O5-Co1-O1, N1-Co1-N1A, O5A-Co1-O1A are 172.73(6)°, 163.64(8)° and 172.73(6)° respectively, deviating from 180.00°, further indicating that the geometries around each metal center all display distorted octahedral. In complex **1**, The bonds length of Co-N 0.21232(15) nm are longer than that of Co-O1 0.21041(13) nm and Co-O5 0.20838(14) nm, indicating that the strength of Co (Ⅱ) ion coordinated with oxygen atoms from MPA^- ligand/ H_2O molecules is stronger than that of nitrogen atoms from MPA^- ligand; while opposite case is found

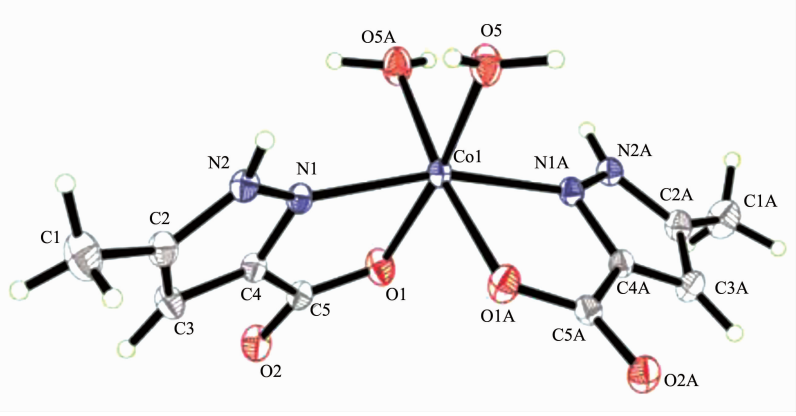

Symmetry code: A: 1/3+*x*−*y*, 2/3−*y*, 1/6−*z*

Fig.1 Coordination environment of Co^{2+} ion in **1**

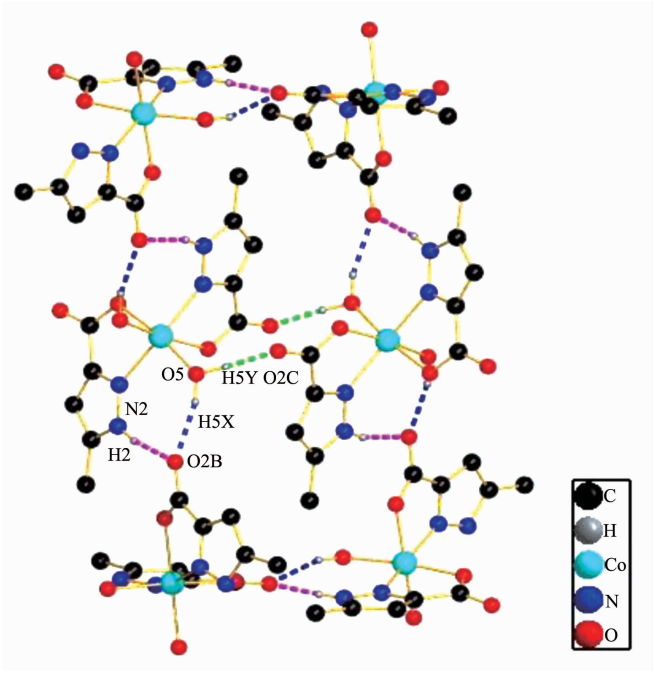

Symmetry codes: B: 2/3−*y*, 1/3−*x*, −1/6+*z*; C: 2/3−*x*+*y*, 1/3+*y*, −1/6+*z*

Fig.2 Hydrogen bonding interactions in complex **1**. Only hydrogen atoms involved in the hydrogen bonds are shown. Hydrogen bonds are indicated by dash lines

in **2** [Ni-N 0.206 6(3) nm, Ni-O1 0.207 4(2) nm, Ni-O3 0.206 8 (2) nm]. The lengths of M-O and M-N bonds around the M(Ⅱ) atom are comparable with those observed in other complexes[39]. As a bidentate ligand, the MPA^- anion chelates one M(Ⅱ) atom with a pyrazole N atom and a carboxyl O atom to form a five membered ring of M1-O1-C5-C4-N1. The bond lengths of N1-N2, C2-N2, C2-C3, C3-C4, C4-N1 in pyrazole ring in **1** and **2** are similar to the values seen in mononuclear complex $[M(MPA)_2(Im)_2\cdot 2H_2O]$ (MPA= 5-methyl-1*H*-pyrazole-3-carboxylate; Im=midazole; M= Co or Ni)[31].

In addition, there are two types of intermolecular hydrogen bonds in both of them: (i) hydrogen bonds between the oxygen (donor) from lattice water and oxygen (acceptor) from MPA^- ligand: O5-H5Y⋯O2C, O5-H5X ⋯ O2B; (ii) hydrogen bonds of an uncoordinated nitrogen (donor) of MPA^- ligand with oxygen (acceptor) from MPA^- ligand: N2-H2⋯O2B, as shown in Fig.2. The neighbouring components $[Co(MPA)_2(H_2O)_2]$ connect each other to form an interesting 3D microporous framework with hexagonal channels via two types of hydrogen bonding interactions mentioned above (Fig.3). The role of the hydrogen bonds in complex **2** is the same as in complex **1** (see Supplementary materials Figures S3-5). The length and angles of the hydrogen bonds for **1** and **2** are listed in Tables 3. PLATON shows that the effective volume for the inclusion is about 0.201 9 nm^3 per unit cell, comprising 3.3% of the crystal volume of **1**. Similarly, for complex **2**, the effective volume in the unit cell is 0.187 2 nm^3, which accounts for 3.1% of the crystal volume.

2.3 Thermogravimetric analyses

In order to examine the thermal stabilities of these compounds, the thermogravimetric analyses were carried out from ambient 25 ℃ to 800 ℃ under nitrogen (see Supplementary materials Figures S6-7). For complex **1**, the first weight loss of 9.48% between 210 ℃ and 226 ℃ is attributed to the loss of two coordinated water molecules (Calcd.:10.42%). The second degradation stage is in the range of 226-232 ℃ with mass loss of 35.39%, corresponding to the loss of one MPA^- ligand (Calcd.:36.23%). The decomposition of the remaining component $[Co(MPA)]^+$ starts above 232 ℃, and finally degrades to CoO with

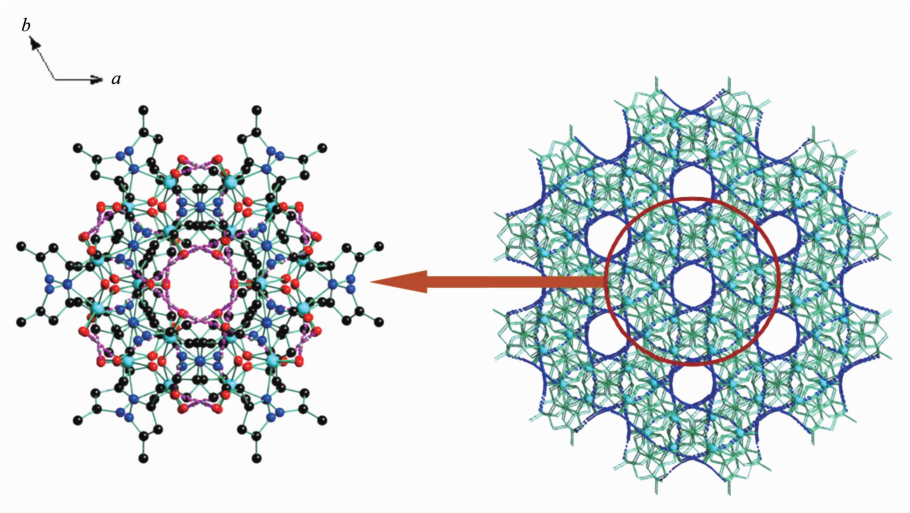

Fig.3 (a) A portion of network architecture in **1** viewed along the c axis; (b) Perspective view of the 3-D supermolecular structure with hexagonal channels of **1**. Only hydrogen atoms involved in the hydrogen bonds are shown. Hydrogen bonds are indicated by dash lines

a loss of 46.74% (Calcd.:46.18%). Complex **1** begins to decompose at 210 ℃, showing it has higher thermal stability and its microporous framework is maintained up to 210 ℃, which is mainly attributable to the strong hydrogen-bonding interactions. For complex **2**, the first weight loss of 47.86% which occurred from 201 to 389 ℃, corresponding to the loss of two coordinated water molecules and one MPA^- ligand (Calcd.:46.70%). Above 389 ℃, the remaining material $[Ni(MPA)]^+$ gradually degrades to NiO with a loss of 22.94% (Calcd.:21.71%).

2.4 Luminescent properties

The luminescent behaviors of free HMPA, **1**, and **2** were investigated in the solid state at room temperature (Supplementary Supplementary materials Figure S8). Complex **1** and **2** exhibit luminescence with emission maxima at 438, and 441 nm upon excitation at 331nm, respectively, and these emissions may be assigned to the intraligand (π-π^*) transfer since a similar emission was observed at 440 nm for the free ligand upon excitation at 331nm. Meanwhile, it is clear that the complex **1** and **2** exhibit weaker emissions compared with the free HMPA ligand, this kind of quenching phenomenon should be related to the ligand-field transitions (d-d)[40-41].

2.5 Electrochemical property

The redox behaviors of complexes were studied by cyclic voltammetry (CV) in aqueous solution, the concentration of $[Co(MPA)_2(H_2O)_2]$(**1**) and $[Ni(MPA)_2(H_2O)_2]$ (**2**) were all 0.5 mmol·L^{-1}. Cyclic voltammogram of the complexes are shown in Figures 4 and 5, during scanning from −1.100 to 1.100 V in

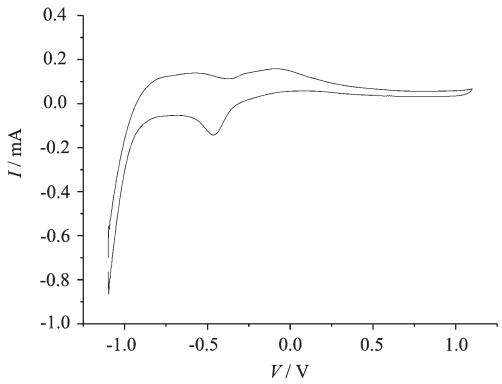

Fig.4 Cyclic voltammogram curve of complex **1**

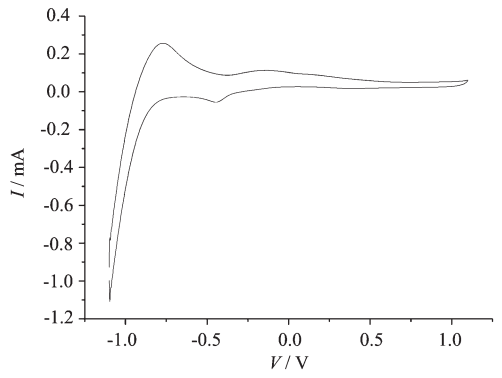

Fig.5 Cyclic voltammogram curve of complex **2**

100 mV·s^{-1}, the cyclic voltammogram curve of both **1** and **2** only have one pair of oxidation-reduction peak, which corresponds to M(Ⅱ)/M(Ⅲ) (**1**: M=Co; **2**: M=Ni) redox process [42]. For **1**, E_{pa}=−0.09 V, E_{pc}=−0.46 V, ΔE=0.37 V, $E_{1/2}$=−0.28 V; For **2**, E_{pa}=−0.138 V, E_{pc}=−0.445 V, ΔE=0.31 V, $E_{1/2}$=−0.29 V. The results show that electron transfer of M (Ⅱ) between M (Ⅲ) in electrolysis is a quasi-reversible process.

3 Conclusions

In conclusion, two new complexes $[M(MPA)_2(H_2O)_2]$ (**1**: M=Co; **2**: M=Ni) with higher thermal stability have been successfully synthesized. The microporous frameworks of **1** and **2** are stable up to 210 ℃ and 201 ℃ respectively. The monomeric components $[M(MPA)_2(H_2O)_2]$ are connected by intermolecular hydrogen bonds to form a three-dimensional architecture with hexagonal channels, indicating that the intermolecular hydrogen bond plays an important role in the thermal stability and the assembly of these high-dimensional supramolecular architectures. Cyclic voltammogram of the complex shows that electron transfer of M (Ⅱ) between M (Ⅲ) (M =Co, Ni) in electrolysis is a quasi-reversible process.

References:

[1] Barbour L J, Orr G W, Atwood J L. *Nature*, **1998**,**393**(18):671-673

[2] Liu Q, Yu L, Wang Y, et al. *Inorg. Chem.*, **2013**,**52**:2817-2822

[3] Chakrabarty R, Mukherjee P S, Stang P J. *Chem. Rev.*, **2011**,**111**:6810-6918

[4] Allendorf M D, Bauer C A, Bhakta R K, et al. *Chem. Soc. Rev.*, **2009**,**38**:1330-1352

[5] Prins L J, Jong F D, Timmerman P, et al. *Nature*, **2000**,**408**(9):181-184

[6] Knoll J D, Arachchige S M, Wang G, et al. *Inorg. Chem.*, **2011**,**50**:8850-8860

[7] Li J R, Kuppler R J, Zhou H C. *Chem. Soc. Rev.*, **2009**,**38**:1477-1504

[8] ZHU En-Jing(朱恩静), LIU Qi(刘琦), CHEN Qun(陈群), et al. *Chinese J. Inorg. Chem.* (*Wuji Huaxue Xuebao*), **2008**,**24**(9):1428-1433

[9] Xu Q, Zou R Q, Zhong R Q, et al. *Cryst. Growth Des.*, **2008**,**8**(7):2458-2463

[10]ZHANG Yan-Peng(张艳朋), CHENG Mei-Ling(程美令), ZHU En-Jing(朱恩静), et al. *Chinese J. Struct. Chem.* (*Jiegou Huaxue*), **2011**,**30**(7):987-994

[11]LI Xiu-Mei(李秀梅), JI Jian-Ye (纪建业), NIU Yang-Ling (牛艳玲), et al. *Chinese J. Inorg. Chem.* (*Wuji Huaxue Xuebao*), **2012**,**28**(8):1712-1716

[12]NI Zhong-Hai (倪中海), NIE Jing (聂景), LI Guo-Ling (李国玲), et al. *Chinese J. Inorg. Chem.* (*Wuji Huaxue Xuebao*), **2012**,**28**(2):411-416

[13]Liu C B, Gong Y N, Chen Y, et al. *Inorg. Chim. Acta*, **2012**,**383**:277-286

[14]Lee Y H, Kubota E, Fuyuhiro A, et al. *Dalton Trans.*, **2012**,**41**:10825-10831

[15]Zhuang W J, Zheng X J, Li L C, et al. *CrystEngComm.*, **2007**,**9**:653-667

[16]Kim H, Das S, Kim M G, et al. *Inorg. Chem.*, **2011**,**50**:3691-3696

[17]Yan S H, Li X X, Zheng X J. *J. Mol. Struct.*, **2009**,**929**:105-111

[18]Hui Y Y, Shu H M, Hu H M, et al. *Inorg. Chim. Acta*, **2010**,**363**:3238-3243

[19]Nagaraja C M, Haldar R, Maji T K, et al. *Cryst. Growth Des.*, **2012**,**12**:975-981

[20]Rosado P J, Senge K R. *J. Coord. Chem.*, **2011**,**64**(1):186-193

[21]Wang L D, Tao F, Chen M L, et al. *J. Coord. Chem.*, **2012**,**65**(6):923-933

[22]Chandrasekhar V, Thirumoorthi R. *Organometallics*, **2009**,**28**:2096-2106

[23]Li Q Y, Chen D Y, He M H, et al. *J. Solid State Chem.*, **2012**,**190**:196-201

[24]Fang R Q, Zhang X M. *Inorg. Chem.*, **2006**,**45**:4801-4810

[25]Noguchi R, Sugie A, Hara A, et al. *Inorg. Chem. Commum.*, **2006**,**9**:107-110

[26]WANG Qing-Hua(王庆华), YU Li-Li(于丽丽), LIU Qi(刘琦), et al. *Chinese J. Inorg. Chem.* (*Wuji Huaxue Xuebao*), **2011**,**27**(5):989-995

[27]Yan B, Capracotta M D, Maggard P A, et al. *J. Coord. Chem.*, **2008**,**61**:1615-1621

[28]Huang Y, Yan B. *J. Coord. Chem.*, **2008**,**61**(10):1615-1621

[29]Li Z P, Xing Y H, Zhang Y H, et al. *J. Coord. Chem.*, **2009**,**62**(4):564-576

[30]Hu F L, Yin X H, Mi Y, et al. *Inorg. Chem. Commum.*, **2009**,**12**:1189-1192

[31]HAN Wei(韩伟), CHENG Mei-Ling(程美令), LIU Qi(刘琦),

et al. *Chinese J. Inorg. Chem.* (*Wuji Huaxue Xuebao*), **2012**,**28**:1997-2004

[32]He X, Lu C Z, Yuan D Q. *Inorg. Chem.*, **2006**,**45**:5760-5766

[33]Zhang Z J, Wojtas L, Zaworotko M J. *Cryst. Growth Des.*, **2011**,**11**:1441-1445

[34]Crane J D, Fox O D, Sinn E. *J. Chem. Soc. Dalton Trans.*, **1999**:1461-1465

[35]Sheldrick G M. *SHELXTL*-97, *Program for Crystal Structure Solution*, University of Gttingen, Gttingen, Germany. **1997**.

[36]Nakamoto K. *Infrared and Raman Spectra of Inorganic and Coordination Compounds*. 4*th Ed*. New York: John Wiley and Sons Inc., **1986**.

[37]Liu Q, Li B L, Xu Z, et al. *Transition Met. Chem.*, **2002**,**27**:786-789

[38]Liu Q, Li B L, Xu Z, et al. *J. Coord. Chem.*, **2003**,**56**(9):771-777

[39]An C X, Lu Y C, Shang Z F, et al. *Inorg. Chim. Acta*, **2008**,**361**:2721-2730

[40]Pan Z R, Song Y, Jiao Y, et al. *Inorg. Chem.*, **2008**,**47**:5162-5168

[41]Zhao J, Wang X L, Shi X, et al. *Inorg. Chem.*, **2011**,**50**:3198-3205

[42]YU Li-Li(于丽丽), LIU Qi(刘琦), XI Hai-Tao(席海涛), et al. *Chinese J. Inorg. Chem.* (*Wuji Huaxue Xuebao*), **2010**,**26**(4):621-626